ELSEVIER

Thermochimica Acta 337 (1999) 27–38

thermochimica acta

www.elsevier.com/locate/tca

Sequential flow injection analysis based on calorimetric detection

A. Wolf, A. Weber, R. Hüttl, J. Lerchner*, G. Wolf

Institute of Physical Chemistry, TU Bergakademie Freiberg, Leipziger Straße 29, D-09596 Freiberg, Germany

Received 18 May 1999; accepted 8 June 1999

Abstract

A calorimetrically based sequential flow injection method with enzyme catalyzed reactions is proposed and demonstrated. In contrast to multi-detection devices with immobilized enzymes miniaturized flow-through reaction calorimeters are used as sensing device with independent substrate and toggled enzyme solution flows. From the sequence of the heat power signals information about composition of the substrate is obtainable. A reasonable application of the method requires miniaturized calorimeters. Different constructions of flow-through reaction calorimeters based on silicon chips with integrated thermopiles as heat power transducers have been analyzed with respect to their sensitivities and mixing behavior. As an application the analysis of saccharides containing mixtures is discussed.

Keywords: Flow-through calorimeter; Thermopile silicon chip; Flow injection analysis; Enzyme catalyzed reactions; Saccharides

1. Introduction

With the development of the enzyme thermistor by Danielsson and Decristofero [1] calorimetric techniques have evoked considerable attention in the area of biosensors and have been applied for the determination of a wide variety of substances like glucose, urea or penicillin. Applying integrated circuit technology and micromachining techniques enzyme thermistors could be down-scaled to the millimeter range. For example, a thermopile-based microsensor developed by Xie et al. [2] consists of a quartz chip with a deposited polysilicon layer. The integrated thermopile was manufactured by ion implantation, pattering of the silicon layer and additional partly metalization through aluminum vapor deposition. A silicon rubber membrane forms a microchannel and serves as seal between chip and a plexiglass cover. Enzyme containing beads are charged into the microchannel. A thermistor based micro-device [3] allows the simultaneous determination of two substrates. It is composed of a quartz transducer chip with five thermistors located along a microchannel which is etched into the chip. The regions between two thermistors are charged with two different enzymes which are covalently immobilized on NHS-activated (*N*-hydroxy succinimide) agarose beads. The serial partitioning of a chip into several discrete detection regions with different immobilized enzymes leads to the idea of a thermometric flow injection method. The feasibility for such an approach was demonstrated by Xie et al. [4] analyzing the dual analytes urea/penicillin and urea/glucose. The simultaneous determination of multiple analytes is an important area in clinical diagnosis as well as in on-line monitoring in a process environment.

*Corresponding author. Tel.: +49-3731-39-2125; fax: +49-3731-39-3588

E-mail address: lerchner@erg.phych.tu-freiberg.de (J. Lerchner)

0040-6031/99/$ – see front matter
PII: S0040-6031(99)00170-7

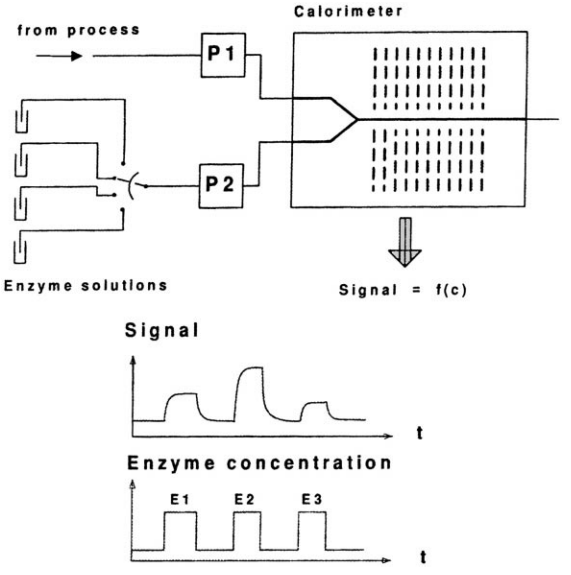

Fig. 1. Scheme of an arrangement for sequential flow injection analysis applying a miniaturized flow-through reaction calorimeter as detector and enzyme catalyzed reactions (P1, P2: pumps; E1, E2, E3: enzyme concentration pulses; Signal: heat power signals regarding to the reaction pulses).

The serial immobilization of several enzymes onto one chip is concatenated with some inflexibility. Moreover, difficulties as thermal carryover and different reaction conditions have to be noticed. Therefore, we propose a flow injection method with a miniaturized flow-through reaction calorimeter as sensing device. Applying a flow-through reaction calorimeter a substrate flow consisting of a mixture of several analytes can be sequentially combined with solutions of appropriate enzymes (see. Fig. 1). Every pulse of the corresponding enzyme solution produces a heat power signal. From the sequence of the signals the composition of the substrate solution should be available. The advantage of the higher flexibility is paid by an increased consumption of enzyme solution. The miniaturization of the calorimeter and the application of micro-pumps is therefore an unalterable prerequisite for a practical use of this method. Further, the reaction conditions should be similar to avoid additional buffering operation during the analysis. As a consequence, our work was divided into two parts. On one hand, we have studied suitable reaction systems, whereby our attention was focused to the thermal sensitivities of the reactions and the optimization of the reaction conditions. The thermal sensitivities were determined by means of a conventional flow-through calorimeter. On the other hand, first investigations with miniaturized devices were performed.

2. Analysis of a saccharide containing mixture using enzyme catalyzed reactions

2.1. Calorimetric measurements

The measurements, which are discussed in the following, were carried out by means of a Micro-DSC II from Setaram with a circulation mixing vessel (31/1530). This vessel has two inlet channels, through which two liquids can be injected, and one outlet. To inject the liquids, we employed two peristaltic pumps "Perimax 12" (Spetec). In a temperature prestabilizer loop, the temperature of the liquids are adjusted to the temperature of the calorimeter. All measurements has been performed at 25°C. Then the inlet liquid flows are forced by special obstacles in the flow channel to improve mixing. The heat power signals were monitored by a data aquisition system [5].

Into one of the inlet tubes a permanent flow of substrate solution was injected. The second inlet was alternately switched between substrate and enzyme solution or a sample loop was used to inject defined pulses of enzyme solution. The flow rates for both channels were equal in each case.

The following enzymes we used: glucose oxidase (EC 1.1.3.4) from Aspergillus niger, approx. 180 U mg^{-1} (Biozyme); catalase (EC 1.11.1.6) from Aspergillus niger, lyophil., approx. 2000 U mg^{-1} (Serva); invertase (EC 3.2.1.26) from yeast, approx. 380 U mg^{-1} (Boehringer Mannheim); α-glucosidase (EC 3.2.1.20) from yeast, lyophil., approx. 100 U mg^{-1} (Serva); hexokinase (EC 2.7.1.1) from yeast overproducer, lyphil., approx.>70 U mg^{-1} (Boehringer Mannheim).

The saccharides sucrose (Merck), maltose (Serva), D(+)-glucose and D(−)-fructose (Fluka) were of the grade "extra pure" and the ATP-Na_2-salt (Serva) too.

All other chemicals were of analytical grade.

2.2. Reaction systems

As model system for the application of a calorimetrically based sequential flow injection analysis tech-

nique we studied the calorimetric detection of the monosaccharides D-glucose and D-fructose and the disaccharides sucrose and maltose in pure and mixed solutions.

1. For detection of sucrose we used invertase (EC 3.2.1.26). This enzyme does not show activity for any of the other applied saccharides [6,7].

$$\text{sucrose} + H_2O \overset{\text{invertase}}{\rightarrow} \text{fructose} + \text{glucose}$$

2. For analyzing glucose we used the enzyme glucose oxidase (EC 1.1.3.4) coupled with catalase (EC 1.11.1.6). This reaction is high specific for β-D-glucose [6–8]. But it consumes oxygen and this will limit the substrate turnover depending on the amount of dissolved oxygen in the solution. These two enzymes are very flexible regarding the pH value and the buffer substances.

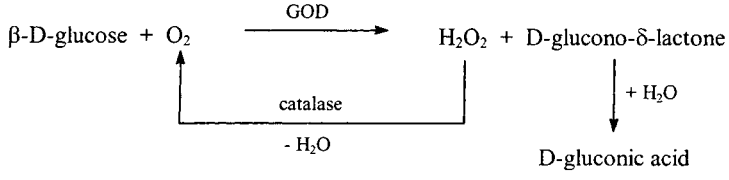

3. The enzyme α-glucosidase (EC 3.2.1.20) was applied for analyzing maltose. But α-glucosidase splits sucrose too and it will be inhibited by the buffer substance TRIS. The reaction enthalpies for these reactions are very low [6–9].

$$\text{maltose} + H_2O \overset{\alpha\text{-glucosidase}}{\rightarrow} 2\,\alpha\text{-D-glucose}$$

$$\text{sucrose} + H_2O \overset{\alpha\text{-glucosidase}}{\rightarrow} \alpha\text{-D-glucose} + \text{fructose}$$

4. We used hexokinase (EC 2.7.1.1) from yeast for detection of D-fructose. For that ATP^{4-} and Mg^{2+} are necessary as cofactors [6–9]. The ATP-Na_2-salt was added to the enzyme solution, while $MgCl_2$ was included in the buffer solution used for the substrate solution and the enzyme solution. Otherwise the effect of dilution of the $MgCl_2$ would be too large. It proved as advantageous to dissolve the hexokinase and the ATP-salt separately and mix them only immediately before injection. The hexokinase catalyzes the transfer of a phosphate group from ATP to water as well as to the hydroxyl group of glucose or fructose but with an extremely lower rate [10,11].

$$\text{fructose} + ATP^{4-} \overset{\text{hexokinase}}{\underset{Mg^{2+}}{\rightarrow}} \text{fructose-6-phosphate}^{2-} + ADP^{3-} + H^+$$

$$\text{glucose} + ATP^{4-} \overset{\text{hexokinase}}{\underset{Mg^{2+}}{\rightarrow}} \text{glucose-6-phosphate}^{2-} + ADP^{3-} + H^+$$

2.3. Results of single analyte detection

In a first step, enzyme reactions with only one saccharide in the substrate solution have been investigated.

For analyzing a mixture of various substrates using a sequential flow injection analysis technique, it is desirable to carry out all enzyme reactions under the same reaction conditions (buffer system, buffer concentration, pH value, concentration of cofactors, flow rate, temperature). But in many cases this would not be possible in practice. Problems with needed cofactors, inhibition effects, stability and activity of enzymes and cofactors can arise. Therefore, it is required to find such conditions under which as many as possible reactions are practicable – not necessarily with the maximum of reaction rate.

As mentioned above the measurement equipment allows to add the enzyme solution permanently to give

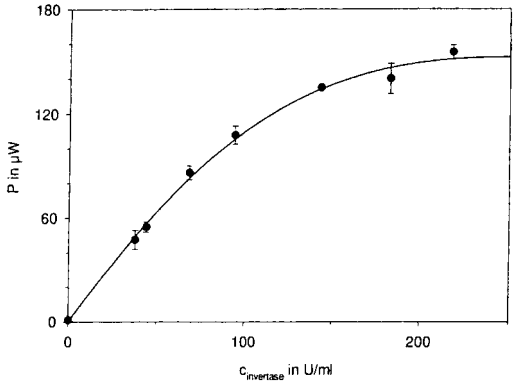

Fig. 2. Dependence of the steady state heat power on the enzyme concentration for the invertase catalyzed sucrose inversion ($c_{sucrose} = 10$ mmol l^{-1}; $v = 14$ ml h^{-1}).

steady state heat power signals or to inject enzyme solution pulses with heat power pulses as a result. In order to save time and expensive substances (enzymes) for the analytical application it is better to work with enzyme impulses than with permanent inputs. In the case of impulse signals both peak heights and peak areas were determined. The peak heights and the peak areas correspond to the maximum heat power and the impulse heat amount. The comparison of the results of steady state and impulse measurements as depicted in Fig. 2 points out that a sample loop with a volume of 1 ml yields peak heights near the steady state signal values.

The slope of the signal parameter vs. saccharide concentration curves are interpreted as analytical sensitivity of the method for the particular saccharide.

For all studied reaction systems the increasing of the flow rate in the range from 7 up to 16 ml h^{-1} (for every input channel) causes only a slight increase of the steady state signal. Therefore, all experiments were carried out with the same flow rate of 10 ml h^{-1}.

In Table 1 the molar reaction enthalpies, the used buffer systems, the concentrations of enzyme and substrates for all reaction systems are summarized. Also the sensitivities regarding to peak height and peak area are listed.

2.3.1. Sucrose+invertase

Fig. 3 shows the dependence of the steady state power on the enzyme concentration at constant concentration of sucrose and flow rate. For all the following measurements we have chosen an invertase concentration of 90 U ml^{-1}.

In the overall range of sucrose concentration (0–200 mmol l^{-1}) we obtained increasing signals as expected (Fig. 2). Up to 15 mmol l^{-1} the dependence of the signals on the substrate concentration is linear with slopes of -8.9 µW l $mmol^{-1}$ and -5.2 mJ l $mmol^{-1}$ regarding peak height and peak area, respec-

Table 1
Summary of the molar reaction enthalpies, the used buffer systems, concentrations of enzyme, the observed range of linearity and the peak height and peak area related sensitivities for the investigated reaction systems (buffers – A: 0.1M acetate, pH 4.6 ; B: 0.1M phosphate, pH 6.9; C: 0.1M TRIS–HCl, pH 8.0; D: 1M TRIS–HCl, pH 8.0 + 0.1M $MgCl_2$)

Reaction system	Buffer	$\Delta_R H$ (kJ mol^{-1}) [9,12]	Enzyme concentration (U ml^{-1})	Linear range (mmol l^{-1})	Sensitivity regarding peak height[c] (µW l $mmol^{-1}$)	Sensitivity regarding peak area[c] (mJ l $mmol^{-1}$)
Sucrose + invertase	A	−15.4	90	15	−8.9	−5.2
Glucose + (GOD/catalase)	A	−225	270/250	1.5	−196	−92
	B	−225				
	C			2	−160	−83
Maltose + α− glucosidase	B	−4	100[b]	40	−0.70	−0.34
Sucrose + α−glucosidase	B		100[b]	20	−2.8	−1.6
Fructose + (hexokinase + ATP)	D	−63[a]	150[b]	20	−24	−7.8
Glucose + (hexokinase + ATP)	D	−74[a]	150[b]	5	−72	−23

[a] Including protonation of buffer.
[b] For unit definition (by the manufacturers) other substrates, buffers, temperatures were used.
[c] In the linear range.

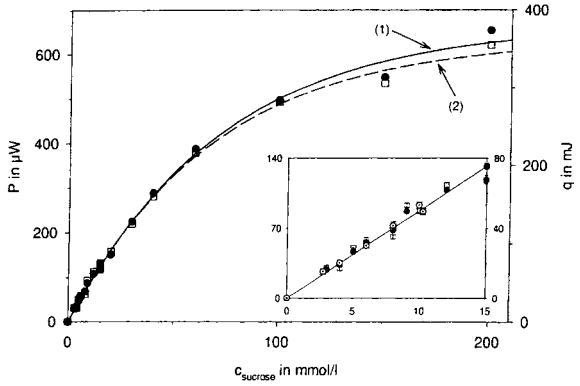

Fig. 3. Comparison of the dependences of the maximum heat power (●/(1)), the impulse heat amount (□/(2)) and the steady state heat power (⊙) on the sucrose concentration for the invertase catalyzed sucrose inversion ($c_{invertase} = 90$ U ml^{-1}; $v = 10$ ml h^{-1}).

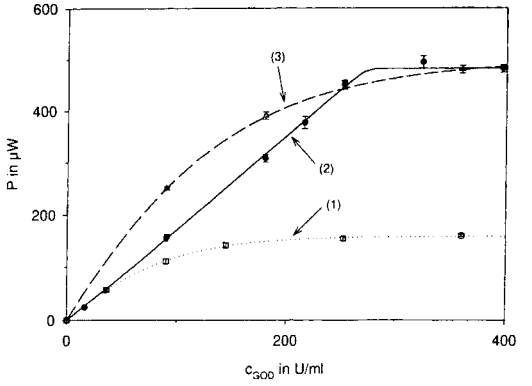

Fig. 4. Dependence of the steady state heat power on the GOD concentration at catalase concentrations of 0 U ml^{-1} (1), 250 U ml^{-1} (2) and 500 U ml^{-1} (3) for the oxidation of glucose catalyzed by GOD and coupled with the catalase catalyzed splitting of H_2O_2 ($c_{glucose} = 4$ mmol l^{-1}; $v = 10$ ml h^{-1}).

tively. The measurable heat power in this range is equivalent to approximately 20% of the heat power for the complete turnover of the supplied substrate. This is due to an incomplete reaction in the mixing cell and incomplete heat exchange between fluid and heat power detector.

2.3.2. Glucose+GOD/catalase

The influence of the enzyme concentration on the heat power signal was investigated performing steady state measurements. In Fig. 4 the results are shown. By addition of catalase the measured heat power is considerable higher than without catalase, because the reaction enthalpy and the available amount of oxygen are increased by the secondary reaction. For the subsequent study of various glucose concentrations we used enzyme concentrations of 270 U ml^{-1} glucose oxidase and 250 U ml^{-1} catalase. The measurements were executed by using the sample loop.

As shown in Fig. 5, we obtained a slope of -160 µW l mmol^{-1} and -83 mJ l mmol^{-1} for peak height and peak area, respectively, in a concentration range of 0–2 mmol l^{-1} and with TRIS buffer pH 8.0. For glucose concentrations above 4 mmol l^{-1} we found constant values of about -400 µW and -210 mJ. Using acetate buffer pH 4.6 which was used for the invertase reaction the linear range is restricted to 1.5 mmol l^{-1} glucose but the values for the measurable heat power are a little higher. A summary of the analyzed concentration ranges, the observed linear

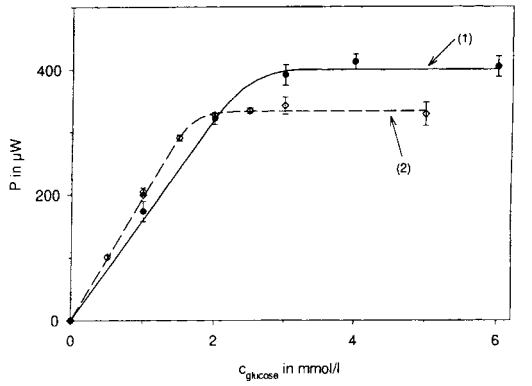

Fig. 5. Correlation between the maximum heat power and the glucose concentration for GOD catalyzed glucose oxidation coupled with the splitting of H_2O_2 catalyzed by catalase in 0.1M TRIS buffer pH 8.0 (1) and in 0.1M acetate buffer pH 4.6 (2) ($c_{GOD} = 270$ U ml^{-1}; $c_{catalase} = 250$ U ml^{-1}; $v = 10$ ml h^{-1}).

ranges and the sensitivities in these ranges are given in Table 1.

2.3.3. Maltose+α-glucosidase

In this case we have chosen an enzyme concentration of approximately 100 U ml^{-1}.

The dependences of the measured heat power and the amount of heat on the concentration of maltose or sucrose show a similar shape like that for the system

sucrose + invertase as described. Because of the very low sensitivities, especially for maltose, the detection limits are relatively high. For the numerical values look at Table 1.

2.3.4. Fructose+hexokinase

We worked with a hexokinase concentration of 150 U ml^{-1} and an ATP^{4-} concentration of 10 mmol l^{-1}.

In the tested range up to 20 mmol l^{-1} fructose we found a linear connection between the substrate concentration and the heat power. This confirms, that the turnover in the mixing cell is far from but complete, because ATP^{4-} and fructose will be converted in the proportion 1 : 1 by this reaction.

For glucose the linear range is limited at about 5 mmol l^{-1} and the detected heat power is three times as high as for fructose in this range. That indicates that glucose reacts under the given conditions with a higher rate than fructose.

2.4. Results for multi-analyte mixtures

2.4.1. Sucrose and glucose

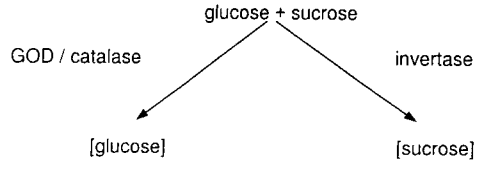

Mixtures containing glucose and sucrose in different proportions were prepared in acetate buffer pH 4.6. Because there are no cross activities, the analysis of glucose with GOD and catalase and of sucrose with invertase were practicable without problems. To determine the concentration of the saccharides in the mixture, repetitive calorimetric measurements with both enzymes have been performed. To calculate the concentrations of the saccharides the sensitivities obtained from the single system measurements were applied.

The experimentally determined concentrations of glucose agree with the applied concentrations better than ±0.1 mmol l^{-1} in the range up to 1.5 mmol l^{-1}. The sucrose concentrations showed deviations of approximately ±0.5 mmol l^{-1} in the range from 2 up to 10 mmol l^{-1}. Nearly the same results were obtained using peak height and peak area related sensitivities. The deviations are independent of the concentration of the additional saccharide, that means no cross sensitivities exist (see Table 2).

In addition, we tested a more complex mixture containing maltose and fructose amongst glucose and sucrose. The concentration of the four saccharides was 10 mmol l^{-1} in the case of sucrose detection and 1.2 mmol l^{-1} for the detection of glucose. Both obtained concentrations were correct.

Furthermore, we analyzed glucose and sucrose in a real sample, i.e. orange-fruit juice drink. We used this juice without any pretreatment, except simple filtering and dilution with buffer in various proportions to reach the linear ranges of the calibration graphs. To check the method, we repeated the measurements after adding known amounts of glucose and sucrose (Table 3). Considering the limits of error the found results correspond with the applied additives.

Thus we could show the suitability of the proposed method for the determination of glucose and sucrose in mixtures.

2.4.2. Maltose and sucrose

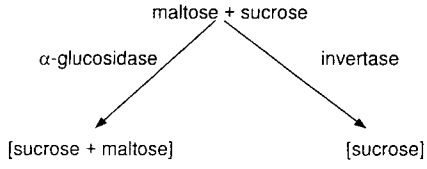

Analyzing maltose with α-glucosidase in presence of sucrose was not possible. The obtained signal agrees with the applied sucrose concentration and is independent of the added maltose concentration, even if the latter was some times as high as the first.

2.4.3. Glucose and fructose

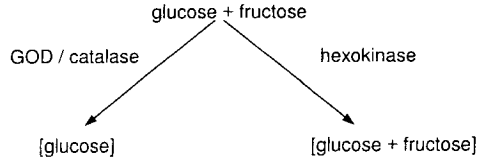

Table 2
Results of analyzing sucrose and glucose in mixtures (c_{theor}: applied concentration; c_{exp}: experimentally determined concentration)

Applied substrate concentration		Determined substrate concentration and deviation from the applied concentration			
c_{theor} (mmol l^{-1})		Calculation regarding peak height		Calculation regarding peak area	
		c_{exp} (mmol l^{-1})	$c_{exp} - c_{theor}$ (mmol l^{-1})	c_{exp} (mmol l^{-1})	$c_{exp} - c_{theor}$ (mmol l^{-1})
Glucose	2.0	1.7	−0.3	2.1	+0.1
Sucrose	10.0	10.1	+0.1	11.2	+1.2
Glucose	1.5	1.5	0.0	1.7	+0.2
Sucrose	6.0	5.9	−0.1	6.9	+0.9
Glucose	1.5	1.5	0.0	1.6	+0.1
Sucrose	6.0	5.1	−0.9	5.7	−0.3
Glucose	0.4	0.4	0.0	0.4	0.0
Sucrose	2.0	2.1	+0.1	2.4	+0.4
Glucose	1.0	0.9	−0.1	1.0	0.0
Sucrose	6.0	5.3	−0.7	6.0	0.0
Glucose	0.4	0.3	−0.1	0.4	0.0
Sucrose	10.0	10.4	+0.4	10.7	+0.7
Glucose	1.5	1.4	−0.1	1.5	0.0
Sucrose	2.0	1.5	−0.5	1.8	−0.2
Glucose	1.5	1.4	−0.1	1.6	+0.1
Sucrose	10.0	8.8	−1.2	9.8	−0.2

Table 3
Recovery of sucrose and glucose in a real orange-fruit juice drink

Dilution (v juice/v solution)	Substrate	Additive (mmol l^{-1})	Determined substrate concentration[a] (mmol l^{-1})	Recovered additive[a] (mmol l^{-1})
0.01	Glucose	–	0.76 ± 0.01	–
		0.40	1.13 ± 0.01	0.37 ± 0.02
0.05	Sucrose	–	7.5 ± 0.3	–
		5.00	12.2 ± 0.6	4.8 ± 0.9

[a] The given errors consist only of the standard deviations of repetitive measurements. They do not include the error of the sensitivity calculated from calibration graphs.

These two saccharides cannot be determined in the same buffer system, because for the hexokinase reaction a very high buffer concentration is necessary. But at higher concentrations of the buffer the GOD reaction will be inhibited. However, the glucose can be analyzed in an other suitable buffer, how it is described above.

The hexokinase reaction goes according a very complex mechanism. For glucose, the formation of a ternary complex (hexokinase-saccharide-ATP) following a random-order-mechanism, including a substrate synergism (induced fit) between glucose and ATP, was described and for fructose a similar mechanism is to be supposed. And both glucose and fructose

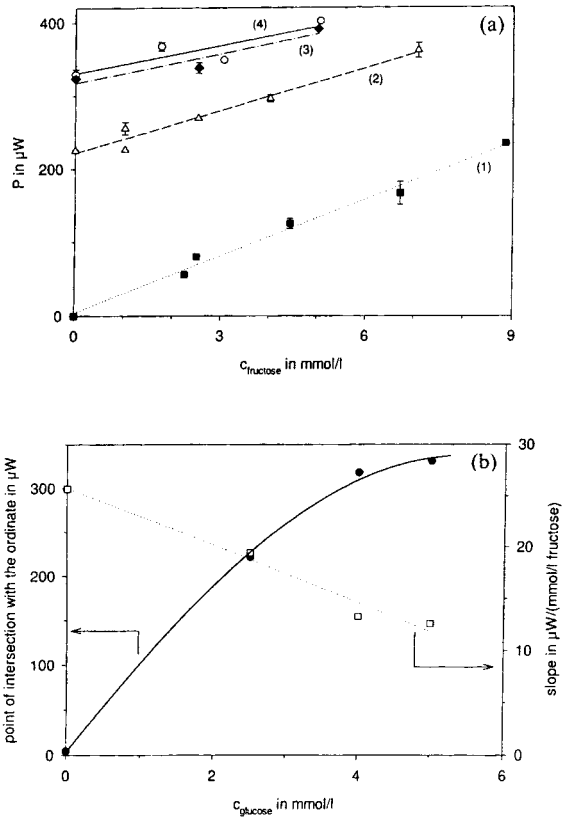

Fig. 6. (a) Dependence of the maximum heat power on the fructose concentration at glucose concentrations of 0 mmol l^{-1} (1), 2.5 mmol l^{-1} (2), 4.0 mmol l^{-1} (3) and 5.0 mmol l^{-1} (4) for the hexokinase catalyzed phosphorylation of glucose and fructose in mixtures ($c_{hexokinase} = 150$ U ml^{-1}; $c_{ATP} = 10$ mmol l^{-1}; $v = 10$ ml h^{-1}); (b) correlation between the parameters of the straight lines from (a) and the glucose concentration.

compete for enzyme and cofactor. The values of the Michaelis constant for glucose, fructose and ATP are in the same range and the concentration of Mg^{2+} has an influence on the reaction rate too [10–12]. At higher glucose concentrations inhibition by the reaction product occurs. Moreover, in the following reaction the buffer substance TRIS is protonated, which results in a rise of the exothermic signal [13]. Because of all these facts it seems impossible to use a kinetic model for calculation of the fructose concentration from the detected heat power.

But for any glucose concentration we found a linear correlation of the maximum heat power with the fructose concentration (see Fig. 6(a)). The point of intersection with the axis of ordinate and the slope of the straight lines depend on the glucose concentration (Fig. 6(b)). For an analytical application it should be possible to determine the dependence of slope and intercept on the glucose concentration experimentally. And with these parameters the fructose concentration is calculable from the heat power signal.

3. Miniaturized flow-through calorimeters and their potentials for flow injection analysis

3.1. Construction of miniaturized flow-through calorimeters

A practical application of the above discussed reactions for flow injection analysis requires well adapted and miniaturized flow-through calorimeters. To study the influence of the design parameters of miniaturized flow-through calorimeters on their signal generation behavior, different versions of flow-through calorimeters have been prepared and tested. They differ in the reactor volume, the layout and the size of the inlet and outlet channels and the type of the used temperature transducers. In all cases, the basic parts of the calorimeters are silicon chips with integrated thermopiles. The basic parts of the first two calorimeters (calorimeter 1 and 2) are monolithic integrated silicon thermopile chips manufactured by Xensor Integration (Delft, The Netherlands) [14,15].

Fig. 7 depicts the schemes of both calorimeters. The reaction chamber of calorimeter 1 is made of a

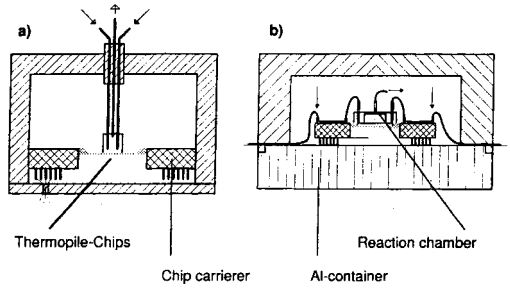

Fig. 7. Schemes of calorimeter 1 (a) and calorimeter 2 (b). Both calorimeters are based on the thermopile chip LCM 2524. Reaction chamber and input channels of calorimeter 2 are milled into a plastic disk.

stainless steel capsule of 40 µl which is glue-bonded onto the sensitive area of the silicon membrane. Capillaries of the same material serve as inlet and outlet for the liquid flow. Due to the poor heat conductivity of the capillaries in comparison with that of the membrane, the decrease of the sensitivity is minor.

In the case of the more compact calorimeter 2, a plastic disk with a thickness of 2 mm is attached to the surface of the silicon chip. The disk contains a cylindrical reaction chamber with a volume of 18 µl and two inlet channels. To improve the thermostating of the input liquid flows, the connecting tubes are contacted to the chip carrier. Both calorimeter arrangements are mounted in a temperature controlled aluminum jacket.

The third calorimeter design combines a free-standing membrane within a silicon frame and a glass chip with wet-etched reaction channel, connected by glue-bonding. This calorimeter has been developed by the group of M. Köhler from the Institute of Physical High-Technology in Jena (Germany) and is described elsewhere [16].

3.2. Characterization of the calorimeters

3.2.1. Analysis of heat transfer

The sensitivity of the discussed flow-through calorimeters depends on the temperature coefficient of the thermopiles, the heat conduction across membrane, tubes and chamber material and it is influenced by mass flow through the calorimeter. To understand the flow rate dependency of the sensitivity and to apply optimal working conditions, the relation between heat transfer by conduction and by forced convection should be known.

The sensitivities can be calculated from the linear slope of the steady-state signal vs. heat power curves. To generate heat power at various flow rates, the integrated electrical heaters were used. Assuming concentrated thermal resistances R_{th}, the heat power balance equation

$$\dot{q}_{el} = \frac{\Delta T}{R_{th}} + 2v\rho c_p \Delta T, \tag{1}$$

yields the expression

$$S_{el} = \frac{dU}{d\dot{q}_{el}} = \frac{\epsilon R_{th}}{1 + 2v\rho c_p R_{th}}, \tag{2}$$

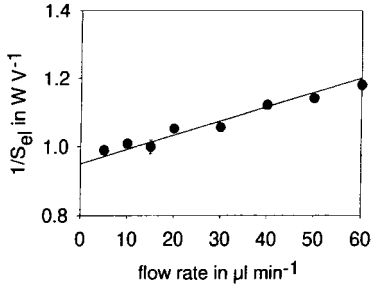

Fig. 8. Flow rate dependency of the sensitivity of calorimeter 1.

for the electrical sensitivity S_{el} with temperature difference ΔT, thermoelectric output voltage $U = \epsilon \Delta T$, fluid density and specific heat capacity ρ and c_p, respectively, thermopower ϵ, and volume flow rate v.

According to the linearized form of Eq. (2)

$$\frac{1}{S_{el}} = \frac{2\rho c_p}{\epsilon} v + \frac{1}{\epsilon R_{th}}, \tag{3}$$

R_{th} and c_p of the fluid should be available from the linear relationship between experimentally determined reciprocal sensitivities and flow rates. Fig. 8 depicts this relationship for calorimeter 1. Slope and intercept yield $R_{th} = 14.3\ K\ W^{-1}$ and $c_p = 5.6\ J\ K^{-1}\ g^{-1}$, respectively. The calculated R_{th} agrees with the value determined at zero flow ($14.1\ K\ W^{-1}$), i.e. the heat conduction is not influenced by the fluid flow. This is in contrast to the behavior of calorimeter 3. As shown in Fig. 9, the above-mentioned assumptions are not realistic at small flow rates. Further, the calculated R_{th} ($150\ K\ W^{-1}$) is markedly higher than that at zero flow ($116\ K\ W^{-1}$). Apparently, there is a heat flow through the glass plate in an opposite direction to the input liquid flow which is more and more eliminated by forced convection.

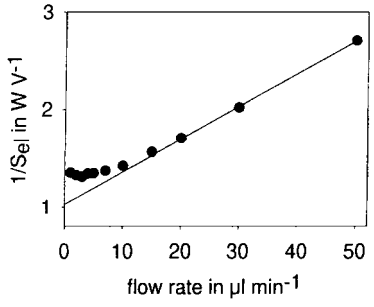

Fig. 9. Flow rate dependency of the sensitivity of calorimeter 3.

3.2.2. Chemical reaction sensitivities

One of the most important problems of the application of chemical reactions in miniaturized flow-through calorimeters evolves from the reduced mixing efficiency of the input liquid flows. The relation of the virtual sensitivity determined using chemical reactions and the joule heating based sensitivity is suitable to quantify the degree of mixing at any given flow rate.

Assuming a "fast" reaction with immediate conversion, the degree of mixing can be defined as

$$D_{\mathrm{mix}} = \frac{(\mathrm{d}n/\mathrm{d}t)_{\mathrm{r}}}{(\mathrm{d}n/\mathrm{d}t)_{\mathrm{in}}} = \frac{\dot{q}_{\mathrm{r}}}{\dot{q}_{\mathrm{max}}} \tag{4}$$

with the rate of reaction $(\mathrm{d}n/\mathrm{d}t)_{\mathrm{r}}$ corresponding to the generated heat power q_{r} and the input rate of reactant $(\mathrm{d}n/\mathrm{d}t)_{\mathrm{in}}$ corresponding to the maximum heat power

$$\dot{q}_{\mathrm{max}} = vc_0\Delta_R H, \tag{5}$$

assuming total mixing and total conversion. Here, c_0 denotes initial concentration, $\Delta_{\mathrm{R}}H$ denotes molar reaction enthalpy. By defining a virtual chemical sensitivity

$$S_{\mathrm{chem}} = \frac{\mathrm{d}U}{\mathrm{d}\dot{q}_{\mathrm{max}}} = \left(\frac{\dot{q}_r}{\dot{q}_{\mathrm{max}}}\right)\frac{\epsilon R_{\mathrm{th}}}{1 + 2v\rho c_{\mathrm{p}}R_{\mathrm{th}}}, \tag{6}$$

the degree of mixing can be determined experimentally by measuring S_{el} and S_{chem}:

$$D_{\mathrm{mix}} = \frac{S_{\mathrm{chem}}}{S_{\mathrm{el}}}. \tag{7}$$

The precondition is, that in joule heating and chemical reaction experiments, the thermal resistances are matching as can be seen by dividing Eq. (2) and Eq. (6).

As a fast test reaction, the protonization of *tris*-(hydroxymethyl)-aminomethane (TRIS) was used. Figs. 10 and 11 show, that the virtual chemical sensitivity is always lower than the joule heating based sensitivity and that the difference increases with increasing flow rates, i.e. the degree of mixing is a function of the flow rate. As one can see from Fig. 12, there are big differences in the degree of mixing between the low-volume calorimeter 3 and both calorimeters 1 and 2 with the larger chamber volumes. This is due to the fact that the rate of mixing is controlled by diffusion only and therefore the volume dependent residence time has a considerable influence.

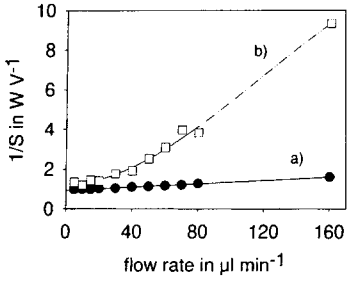

Fig. 10. Comparison of joule heating (a) and virtual chemical (b) sensitivities of calorimeter 1.

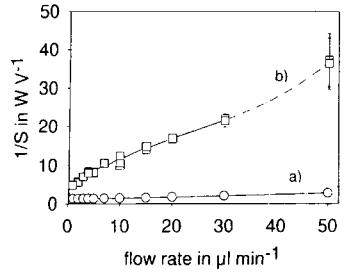

Fig. 11. Comparison of joule heating (a) and virtual chemical (b) sensitivities of calorimeter 3.

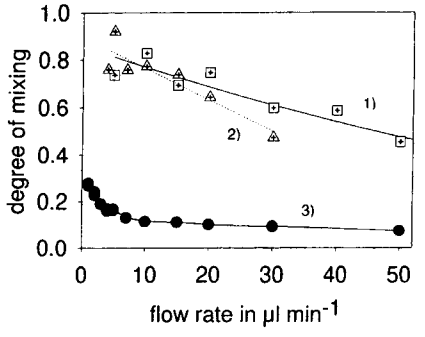

Fig. 12. Degree of mixing of the calorimeters 1 (squares), 2 (triangles) and 3 (circles).

3.3. Monitoring enzyme catalyzed reactions

Fig. 13 shows results of applications of the sucrose inversion reaction to the miniaturized flow-through calorimeter described above. The compared signals are generated by enzyme solution pulses injected into sucrose solution flows of constant concentrations. They correspond to equal concentrations of sucrose (100 mmol l^{-1}) and enzyme activities (90 U ml^{-1}).

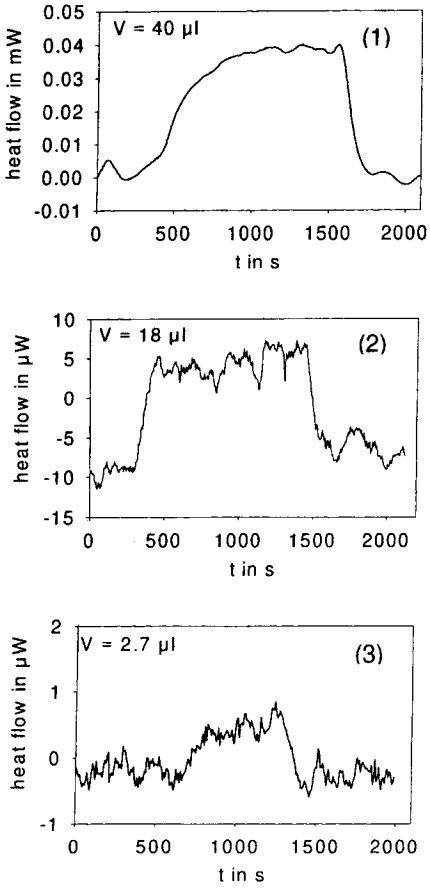

Fig. 13. Heat power signals generated by enzyme solution pulses injected into a continuos flow of sucrose solution: (1) calorimeter 1; (2) calorimeter 2; (3) calorimeter 3.

Obviously, the signal strongly depends on the volume of the reaction chamber. Because the reaction is kinetically controlled, the reduction of the volume and hence the decrease of the residence time not only reduces the mixing efficiency but also the degree of conversion. Therefore, it is very important to optimize the volume of the reaction chamber.

4. Conclusions

Due to the universal nature of the heat power production of chemical reactions, a single flow-through calorimeter can be applied as detector to different sensor reactions without modification. As an alternative to the application of the well-known multi-detection devices with immobilized enzymes, a sequential flow injection analysis technique with independent substrate and toggled enzyme solution flow offers a higher degree of flexibility. Requirements for the construction of appropriate flow through reaction calorimeters arise from the limitations for the enzyme consumption and a necessary residence time. Latter assures sufficient high degrees of mixing and reaction, especially because the reaction is kinetically controlled. Therefore, miniaturized flow-through reaction calorimeters have to be optimized carefully to obtain reasonable sensitivities.

As an application of the proposed calorimetrically based sequential flow injection method, the analysis of different saccharides containing mixtures seems possible in general. But care has to be taken at the selection of the enzymes, because cross sensitivities evoke additional effort for calibrations or restrict the determination of distinct analytes. The application to saccharide mixtures has been tested because of its importance for food industry and biotechnology.

Acknowledgements

This work was funded by the German Research Council (Deutsche Forschungsgemeinschaft) under grant Wo 576/1. We thank M.J. Köhler and M. Zieren (IPHT Jena) for fruitful cooperation.

References

[1] G. Decristofero, B. Danielsson, Anal. Chem. 56 (1984) 263.
[2] B. Xie, M. Mecklenburg, B. Danielsson, O. Öhmann, F. Winquist, Anal. Chim. Acta 299 (1994) 1965.
[3] B. Xie, M. Mecklenburg, B. Danielsson, O. Öhmann, P. Norlin, F. Winquist, Analyst 120 (1995) 155.
[4] B. Xie, K. Ramanathan, B. Danielsson, in: T. Scheper (Ed.), Advances in Biochemical Engineering Biotechnology, Springer, Berlin, 1999, pp. 1–33.
[5] SETARAM; Thermal Analysis in Biochemistry and Pharmacy, Application sheet no. 3, 1994.
[6] H.U. Bergmeyer; Methoden der enzymatischen Analyse, Akademie-Verlag, Berlin, 1970.
[7] Enzyme Handbook, Springer, Berlin, 1994.
[8] Römpp; Chemie Lexikon, 9th ed., Georg-Thieme-Verlag, Stuttgart, New York, 1991/92.

[9] http//:ibm4.carb.nist.gov:8800/enzyme.
[10] W.P. Jencks, Catalysis in Chemistry and Enzymology, Dover, New York, 1969.
[11] A. Fersht, Enzyme Structure and Mechanism, 2nd ed., Freeman, New York, 1985.
[12] T. Palmer, Understanding Enzymes, 4th ed., Prentice Hall, London, 1995.
[13] K. Bohmhammel, R. Hüttl, K. Pritzkat, G. Wolf, Thermochim. Acta 250 (1995) 1.
[14] J. Lerchner, A. Wolf, G. Wolf, J. Thermal Anal. 57 (1999) 241.
[15] A.W. Herwaarden, P. Sarro, Sensors and Actuators 10 (1986) 321.
[16] J.M. Köhler, M. Zieren, Thermochim. Acta 310 (1998) 25.